J. Fluid Mech. (2007), *vol.* 593, *pp.* 453–462.
doi:10.1017/S0022112007008658 Printed in the United Kingdom

On the motion induced in a gas confined in a small-scale gap due to instantaneous boundary heating

A. MANELA[1] AND N. G. HADJICONSTANTINOU[2]

[1]Department of Mathematics, Massachusetts Institute of Technology, Cambridge, MA 02139, USA

[2]Department of Mechanical Engineering, Massachusetts Institute of Technology, Cambridge, MA 02139, USA

(Received 20 May 2007 and in revised form 14 September 2007)

We analyse the time response of a gas confined in a small-scale gap (of the order of or smaller than the mean free path) to an instantaneous jump in the temperature of its boundaries. The problem is formulated for a collisionless gas in the case where the relative temperature jump at each wall is small and independent of the other. An analytic solution for the probability density function is obtained and the respective hydrodynamic fields are calculated. It is found that the characteristic time scale for arriving at the new equilibrium state is of the order of several acoustic time scales (the ratio of the gap width to the most probable molecular speed of gas molecules). The results are compared with direct Monte Carlo simulations of the Boltzmann equation and good agreement is found for non-dimensional times (scaled by the acoustic time) not exceeding the system Knudsen number. Thus, the present analysis describes the early-time behaviour of systems of arbitrary size and may be useful for prescribing the initial system behaviour in counterpart continuum-limit analyses.

1. Introduction

The study of the time response of a fluid confined between two parallel walls and subject to a change in the thermal properties of its boundaries is of fundamental importance in both classical fluid mechanics (Schlichting 1960) and rarefied gasdynamics (Patterson 1971). Essentially, the fluid motion induced in this problem is driven by the mechanism of thermal expansion: temperature changes in the vicinity of the boundary result in density gradients which, in turn, are balanced by the appearance of a velocity field perpendicular to the wall. When the imposed variations at the boundaries persist for a finite period of time, this mechanism acts to bring the fluid to a new state of equilibrium. The problem of gradual change in wall thermal properties was studied in the context of continuum Navier–Stokes gasdynamics in a series of works by Kassoy and co-authors (e.g. Rhadwan & Kassoy 1984; Clarke, Kassoy & Riley 1984). To justify their use of a continuum gas description, these studies assume that the variations of wall properties occur over a finite time period which cannot be shorter than some modest multiple of the characteristic molecular relaxation time scale (the mean free time between molecular collisions for a gas). However, this assumption is not justified in a number of practical applications involving fast processes (Chen 2002). These are encountered, for example, during manufacturing processes where ultrafast (femtosecond to picosecond pulse durations) laser heating is

utilized (Tzou, Beraun & Chen 2002) and are of considerable engineering importance (Tzou 1997). Considering such time scales requires taking into account the molecular response of the gas at the initial stages of the system transient.

The problem of instantaneous wall heating in dilute gases was first treated by Sone (1965) for the case of a semi-infinite expanse. The temperature increase relative to the initial temperature was assumed small and the fluid motion was analysed using the Bhatnagar, Gross and Krook (BGK) model of the Boltzmann equation. Lees (1965) addressed the same problem by assuming a two-sided Maxwellian distribution for the probability density function and applying the method of moments to obtain an approximate solution. Later works have considered the problem in a finite gap. Perlmutter (1967) studied the transient heat transfer through a collisionless gas with a step change in one wall temperature. In his analysis, a set of integral equations for the flux of a general macroscopic quantity was derived and then solved numerically. More recently, Wadsworth, Erwin & Muntz (1993) studied the problem numerically for a wide range of Knudsen numbers (the ratio of molecular mean free path to characteristic flow length scale) using the direct simulation Monte Carlo (DSMC) method. At small Knudsen numbers they compared their results to those obtained using a finite difference scheme of the continuum Navier–Stokes model. Their comparison verifies that, however small the Knudsen number, there always exists an initial transient period where molecular effects are important and cannot be captured by the Navier–Stokes continuum description (Grad 1958).

In this study we consider the problem of a discontinuous change in boundary temperatures of a confined dilute gas. In the following analysis we provide an analytical solution for the molecular distribution function on the basis of the collisionless Boltzmann equation. With this solution we aim to describe, both for fundamental and practical purposes, two classes of applications: first, systems that have characteristic dimensions that are small compared to the molecular mean free path, which are of interest in micro- and nano-scale engineering applications (Ho & Tai 1998; Hadjiconstantinou 2006); second, the early-time response of systems of arbitrary size (Wadsworth *et al.* 1993). The latter may also be useful as a means of providing a quantitative prescription of the system initial transient behaviour for long-time continuum analyses of a variety of thermal processes of practical interest (Wadsworth *et al.* 1993).

In § 2 the microscopic problem for a collisionless gas is analysed assuming small temperature jumps at the walls. In § 3 the results obtained for the hydrodynamic fields are presented and compared with DSMC calculations. It is thus verified that the present analysis provides an accurate description for the initial gas response for times significantly smaller than the molecular collision time and a good approximation for times up to one collision time. Thus, it describes the initial response of systems of arbitrary size. Furthermore, it is demonstrated that the present results capture the late-time behaviour for systems that are much smaller than the molecular mean free path, and, depending on the level of approximation required, provide a satisfactory description for systems of size of the order of the mean free path.

2. Problem formulation and analysis

2.1. *Problem formulation*

We consider a dilute-gas† layer of molecular mass m^* and uniform density ρ_0^* confined between two infinitely long diffusely reflecting walls placed in the (y^*, z^*)-plane at

† Air at standard temperature and pressure satisfies the dilute-gas criteria (Bird 1994).

$x^* = \pm L^*/2$; here, * denotes a dimensional quantity. The gas is initially at rest and in thermodynamic equilibrium with the confining walls at a temperature T_0^*.

At $t^* = 0$ a sudden temperature jump occurs at each of the confining boundaries. We assume that each of these temperature jumps ($\Delta T_\pm^*$ at $x^* = \pm L^*/2$, respectively) is small relative to T_0^* so that the system description may be linearized about its initial equilibrium. To render the problem dimensionless we normalize the position by L^*, the velocity by the most probable molecular speed $U_{th}^* = \sqrt{2R^*T_0^*}$, and the density and temperature by ρ_0^* and T_0^*, respectively. The resulting time scale is thus the acoustic scale $t_a^* = L^*/U_{th}^*$. Here, $R^* = k_B^*/m^*$ is the specific gas constant and k_B^* is Boltzmann's constant. For future reference we define the Knudsen number

$$Kn = l^*/L^*$$

wherein $l^* = m^*/(\sqrt{2}\pi\rho_0^* d^{*2})$ is the molecular mean free path and d^* the 'equivalent' hard-sphere diameter. The molecular collision time is given by $t_c^* = \sqrt{\pi}l^*/(2U_{th}^*)$. The gas state is described by the probability density function

$$f(t, x, \boldsymbol{c}) = F[1 + \epsilon\phi(t, x, \boldsymbol{c})] \tag{2.1}$$

wherein $\boldsymbol{c} = (c_x, c_y, c_z)$ is the vector of molecular velocity, $F = \pi^{-3/2}\exp[-c^2]$ is the equilibrium Maxwellian distribution and $\epsilon = \Delta T_-^*/T_0^* \ll 1$.

Neglecting the effects of molecular collisions, the linearized problem for ϕ is governed by the collisionless Boltzmann equation (Kogan 1969)

$$\frac{\partial\phi}{\partial t} + c_x\frac{\partial\phi}{\partial x} = 0 \tag{2.2}$$

together with the initial condition

$$\phi(t = 0, x, \boldsymbol{c}) = 0 \tag{2.3}$$

and the linearized diffuse boundary conditions

$$\phi(t, x = \mp 1/2, c_x \gtrless 0) = \rho_\pm(t) + \begin{bmatrix} 1 \\ R_\epsilon \end{bmatrix}\left(c^2 - \frac{3}{2}\right). \tag{2.4}$$

$R_\epsilon = \Delta T_+^*/\Delta T_-^*$ specifies the temperature change at the wall $x = +1/2$ and $\rho_\pm(t)$ are yet to be determined (see (2.8), (2.9) *et seq.*).

Given the collisionless approximation, we expect solutions to the above problem to provide a close description of the gas response for $t \ll Kn$ ($t^* \ll t_c^*$) and a reasonable approximation for $t \lesssim Kn$.

2.2. *Problem solution*

Taking the Laplace transform of (2.2) and using (2.3) and (2.4) yields the solution

$$\hat{\phi}(s, x, c_x \gtrless 0, c_y, c_z) = \left[\hat{\rho}_\pm(s) + \begin{bmatrix} 1 \\ R_\epsilon \end{bmatrix}\left(\frac{c^2}{s} - \frac{3}{2s}\right)\right]\exp\left[-\frac{s}{c_x}\left(x \pm \frac{1}{2}\right)\right] \tag{2.5}$$

where s is the Laplace variable and $\hat{}$ denotes the Laplace transform of a function. By inversion of (2.5) we obtain

$$\phi(t, x, c_x \gtrless 0, c_y, c_z) = \rho_\pm(t_\pm) + \begin{bmatrix} 1 \\ R_\epsilon \end{bmatrix}\left(c^2 - \frac{3}{2}\right)U(t_\pm) \tag{2.6}$$

where $U(t)$ is the step function and $t_\pm = t - (x \pm 1/2)/c_x$.

The fields $\rho_{\pm}(t)$ are determined by imposing impermeability conditions at the walls

$$\int_{-\infty}^{\infty} c_x \phi \left(x = \mp \frac{1}{2} \right) F \mathrm{d}\boldsymbol{c} = 0. \tag{2.7}$$

Substituting (2.6) into (2.7) yields a pair of coupled integral equations

$$\rho_- - \int_0^t \frac{\mathrm{d}\rho_+}{\mathrm{d}\tau} \exp\left[-\frac{1}{(t-\tau)^2} \right] \mathrm{d}\tau = \frac{1}{t^2} \exp\left[-\frac{1}{t^2} \right] - \frac{R_\epsilon}{2}, \tag{2.8}$$

$$\rho_+ - \int_0^t \frac{\mathrm{d}\rho_-}{\mathrm{d}\tau} \exp\left[-\frac{1}{(t-\tau)^2} \right] \mathrm{d}\tau = \frac{R_\epsilon}{t^2} \exp\left[-\frac{1}{t^2} \right] - \frac{1}{2}, \tag{2.9}$$

which need to be solved in conjunction with the initial conditions $\rho_+(0) = -1/2$ and $\rho_-(0) = -R_\epsilon/2$. Rewriting this problem in terms of $\sigma = \rho_+ + \rho_-$ and $\delta = \rho_+ - \rho_-$ results in the two uncoupled equations

$$\int_0^t \frac{\mathrm{d}\sigma}{\mathrm{d}\tau} \left\{ 1 - \exp\left[-\frac{1}{(t-\tau)^2} \right] \right\} \mathrm{d}\tau = \frac{R_\epsilon + 1}{t^2} \exp\left[-\frac{1}{t^2} \right] \tag{2.10}$$

and

$$\int_0^t \frac{\mathrm{d}\delta}{\mathrm{d}\tau} \left\{ 1 + \exp\left[-\frac{1}{(t-\tau)^2} \right] \right\} \mathrm{d}\tau = \frac{R_\epsilon - 1}{t^2} \exp\left[-\frac{1}{t^2} \right], \tag{2.11}$$

where $\sigma(0) = -(R_\epsilon + 1)/2$ and $\delta(0) = (R_\epsilon - 1)/2$.

To solve for $\sigma(t)$ we apply the Laplace transform of (2.10) in conjunction with the initial condition to obtain

$$\hat{\sigma}(s) = \frac{R_\epsilon + 1}{2} \left[-\frac{1}{s} + \frac{\mathrm{d}}{\mathrm{d}s} [\ln(1 - 2\hat{J}_1)] \right] \tag{2.12}$$

where

$$\hat{J}_n = \int_0^\infty \frac{1}{t^{n+2}} \exp\left[-\frac{1}{t^2} - st \right] \mathrm{d}t. \tag{2.13}$$

To calculate the inverse transformation we make use of the Taylor expansion ($0 < |\hat{J}_1| < 1/2$ for all s with $\mathrm{Re}\{s\} > 0$)

$$\ln(1 - 2\hat{J}_1) = -\sum_{n=1}^{\infty} \frac{(2\hat{J}_1)^n}{n}$$

which yields

$$\sigma(t) = (R_\epsilon + 1) \left[-\frac{1}{2} + J_0 + \sum_{n=1}^{\infty} 2^n J_1^{(n)} * J_0 \right]. \tag{2.14}$$

The operator $g^{(n)} * h = g * g * \ldots * (g * h)$ denotes n successive convolutions of g with h and

$$g * h = \int_0^t g(t-\tau) h(\tau) \mathrm{d}\tau \, .$$

A similar procedure is followed to obtain $\delta(t)$, yielding

$$\hat{\delta}(s) = \frac{-R_\epsilon + 1}{2} \left[-\frac{1}{s} + \frac{\mathrm{d}}{\mathrm{d}s} [\ln(1 + 2\hat{J}_1)] \right] \tag{2.15}$$

and, upon inversion,

$$\delta(t) = (-R_\epsilon + 1)\left[-\frac{1}{2} - J_0 - \sum_{n=1}^{\infty}(-2)^n J_1^{(n)} * J_0\right]. \tag{2.16}$$

Our numerical calculations indicate that both (2.14) and (2.16) converge after a relatively small number of terms ($n \leqslant 10$) for all $t \lesssim O(1)$. The expressions

$$\rho_+(t) = -\frac{1}{2} + R_\epsilon J_0 + \sum_{n=1}^{\infty}\left[2^{2n} R_\epsilon J_1^{(2n)} * J_0 + 2^{2n-1} J_1^{(2n-1)} * J_0\right], \tag{2.17}$$

$$\rho_-(t) = -\frac{R_\epsilon}{2} + J_0 + \sum_{n=1}^{\infty}\left[2^{2n} J_1^{(2n)} * J_0 + 2^{2n-1} R_\epsilon J_1^{(2n-1)} * J_0\right] \tag{2.18}$$

are then readily obtained.

Once ϕ is known, the $O(\epsilon)$ perturbations of the hydrodynamic fields may be calculated by appropriate quadratures over the molecular velocity space (Kogan 1969). Introducing

$$\Phi_\pm^n = \int_{\pm c_{x_\pm}}^{\infty} c_x^n \exp\left[-c_x^2\right] \mathrm{d}c_x, \quad \Psi_\pm^n = \int_{c_{x_\pm}}^{\pm\infty} \rho_\pm(t_\pm) c_x^n \exp\left[-c_x^2\right] \mathrm{d}c_x \tag{2.19}$$

with $c_{x_\pm} = (x \pm 1/2)/t$, the $O(\epsilon)$ density, x-component velocity, temperature and x-component heat flux (scaled by $\rho_0^* {U_{th}^*}^3$) perturbations are respectively expressed as

$$\rho = \frac{1}{\sqrt{\pi}}\left[\Psi_+^0 - \Psi_-^0 + \Phi_+^2 + R_\epsilon \Phi_-^2 - \tfrac{1}{2}(\Phi_+^0 + R_\epsilon \Phi_-^0)\right], \tag{2.20}$$

$$u_x = \frac{1}{\sqrt{\pi}}\left[\Psi_+^1 - \Psi_-^1 + \Phi_+^3 - R_\epsilon \Phi_-^3 - \tfrac{1}{2}(\Phi_+^1 - R_\epsilon \Phi_-^1)\right], \tag{2.21}$$

$$T = \frac{2}{3\sqrt{\pi}}\left[\Psi_+^2 - \Psi_-^2 + \tfrac{5}{2}(\Psi_+^0 - \Psi_-^0) + \Phi_+^4 + R_\epsilon \Phi_-^4 - \Phi_+^2 - R_\epsilon \Phi_-^2 + \Phi_+^0 + R_\epsilon \Phi_-^0\right], \tag{2.22}$$

$$q_x = \frac{1}{2\sqrt{\pi}}\left[\Psi_+^3 - \Psi_-^3 + \Psi_+^1 - \Psi_-^1 + \Phi_+^5 - R_\epsilon \Phi_-^5 + \tfrac{1}{2}(\Phi_+^3 - R_\epsilon \Phi_-^3) + \tfrac{1}{4}(\Phi_+^1 - R_\epsilon \Phi_-^1)\right] - \tfrac{5}{4} u_x. \tag{2.23}$$

2.3. *Early- and late-time approximations of the hydrodynamic fields*

At early times, due to the fast exponential decay of J_n (the inverse Laplace transform of (2.13)) and the vanishingly small contributions from the convolution terms, both ρ_+ and ρ_- may be approximated by their respective first terms in (2.17) and (2.18):

$$\rho_+ \approx -\tfrac{1}{2} + O(t^{-2}\exp[-t^{-2}]), \qquad \rho_- \approx -\frac{R_\epsilon}{2} + O(t^{-2}\exp[-t^{-2}]). \tag{2.24}$$

Substituting (2.24) into (2.19)–(2.23) yields the early-time approximations

$$\rho \approx \frac{1}{2\sqrt{\pi}}\left[c_{x_+}\exp\left[-c_{x_+}^2\right] + R_\epsilon c_{x_-}\exp\left[-c_{x_-}^2\right] - \frac{\sqrt{\pi}}{2}\left(\gamma(c_{x_+}) + R_\epsilon \gamma(c_{x_-})\right)\right], \tag{2.25}$$

$$u_x \approx \frac{1}{2\sqrt{\pi}}\left[c_{x_+}^2\exp\left[-c_{x_+}^2\right] - R_\epsilon c_{x_-}^2\exp\left[-c_{x_-}^2\right]\right], \tag{2.26}$$

$$T \approx \frac{1}{2\sqrt{\pi}}\left[\frac{1}{3}\left(c_{x_+}^3\exp\left[-c_{x_+}^2\right] + R_\epsilon c_{x_-}^3\exp\left[-c_{x_-}^2\right]\right) + \frac{\sqrt{\pi}}{4}\left(\gamma(c_{x_+}) + R_\epsilon \gamma(c_{x_-})\right)\right] \tag{2.27}$$

$$q_x \approx \frac{1}{2\sqrt{\pi}}\left[\exp\left[-c_{x_+}^2\right]\left(\tfrac{1}{2}c_{x_+}^4 + c_{x_+}^2 + 1\right) - R_\epsilon \exp\left[-c_{x_-}^2\right]\left(\tfrac{1}{2}c_{x_-}^4 + c_{x_-}^2 + 1\right)\right] - \tfrac{5}{4}u_x, \tag{2.28}$$

wherein $\gamma(z) = (2/\sqrt{\pi})\int_z^\infty \exp[-p^2]\mathrm{d}p$ is the complementary error function. Owing to the lack of interaction between walls at $t \ll 1$, expressions (2.25)–(2.28) can also be obtained as a superposition of the local responses of the gas in the vicinity of each wall. The temperature and density fields at short times for the case of a wall in contact with a semi-infinite expanse of gas were first given by Sone (1965).

At late times, applying the final-value theorem to (2.12) and (2.15), we find that

$$\rho_+ \approx -\rho_- \approx \tfrac{1}{4}(R_\epsilon - 1)\,. \tag{2.29}$$

It thus follows that at $t \gg 1$ both density and velocity perturbations vanish while the temperature, $T \approx (1 + R_\epsilon)/2$, and heat flux, $q_x \approx (1 - R_\epsilon)/(2\sqrt{\pi})$, distributions become uniform.

3. Results and discussion

In the following we compare our results to direct Monte Carlo (Bird 1994) solutions of the Boltzmann equation for a hard-sphere gas. The hard-sphere model was chosen owing to its relative simplicity. We expect the actual choice of interaction model to have a small effect on the results obtained, because of the near-collisionless nature of the flow and the small temperature differences studied here. Our simulations are homogeneous in the y- and z-directions; the x-direction is discretized using $n_c = 50$ computational cells for $Kn \geqslant 1$ (and $n_c = 100$ for $Kn = 0.1$), while the time step is chosen to be a small fraction (typically 0.2) of the cell traversal time $L^*/(n_c U_{th}^*)$; 1000 particles per cell are used. The results are ensemble averaged until the desired statistical uncertainty is obtained. In accordance with our problem description, the gas is initially at equilibrium with the common wall temperature T_0^* and diffuse boundary conditions are used. At $t^* = 0$ each wall temperature is changed impulsively and the flow field is followed through to its new equilibrium state. To account for the linearization assumption set in § 2, our simulations are carried out with $\epsilon = 0.02$ and $-1 \leqslant R_\epsilon \leqslant 1$. Note that according to our numerical results nonlinear effects remain relatively small up to $\epsilon \approx 0.1$ for the same range of R_ϵ.

Figure 1 shows the space and time variations of the hydrodynamic perturbation fields (2.20)–(2.23) for the case where the temperature jumps at the walls are equal ($R_\epsilon = 1$). The crosses correspond to DSMC results at $Kn = 10$ and the thin lines mark the late-time collisionless limit (see § 2.3). For this value of R_ϵ, $\rho_+ = \rho_-$ (see (2.8)–(2.9)). It follows that the density and temperature perturbations are symmetric while the velocity and heat flux are antisymmetric about $x = 0$.

At early times ($t \ll 1$) we observe that density and velocity disturbances propagate in a wave-like manner away from the walls with a nearly constant amplitude. At these times, the early-time expressions (2.25)–(2.28) provide approximations that are indistinguishable from the more general solution (2.20)–(2.23). The respective amplitudes of the left- and right-travelling velocity disturbances are predicted by (2.26) to be $1/(2\sqrt{\pi}\mathrm{e})$ and $-R_\epsilon/(2\sqrt{\pi}\mathrm{e})$ while their respective locations are $x = -0.5 + t$ and $x = 0.5 - t$. This is in remarkable agreement with the observed (DSMC) behaviour. At $t \approx 0.2$ the two waves adjoin and at later times the gas approaches its new equilibrium state through a series of decaying waves propagating across the gap. At the latest

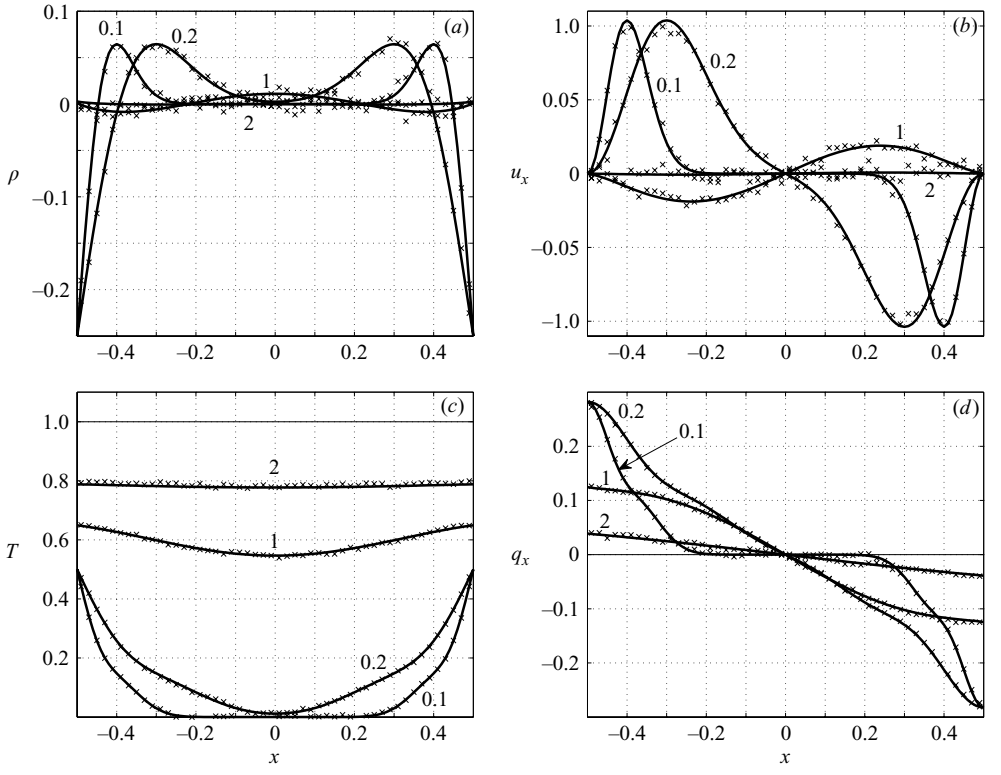

FIGURE 1. (*a*) Density, (*b*) velocity, (*c*) temperature and (*d*) heat-flux perturbation distributions for $R_\epsilon = 1$ and the indicated values of time. The crosses correspond to DSMC results at $Kn = 10$ and the thin solid lines mark the long-time collisionless limit.

time presented ($t = 2$), the density and velocity perturbations are already vanishingly small while the temperature and heat flux are still evolving towards their final values.

In view of the vastly different methods of calculation, the close agreement between the present analysis and DSMC results is gratifying. Furthermore, in contrast to the relatively costly numerical procedure (Hadjiconstantinou *et al.* 2003) in which the appearance of artificial noise is inevitable (see, e.g., the scatter of results for late times in the density and velocity fields), the present exact solution has the evident advantage of requiring very small computational effort.

Figure 2 compares the variation of the hydrodynamic fields (2.20)–(2.23) for $R_\epsilon = -1$ with respective DSMC results at $Kn = 10$. For this case, $\rho_+ = -\rho_-$ and the symmetry properties are reversed compared to those in figure 1. The transient time observed here is longer than in the $R_\epsilon = 1$ case: at the largest value of $t = 4$ presented, none of the fields has yet reached its equilibrium state. When comparing the results obtained with DSMC calculations we find that the agreement at late times is less satisfactory. We note that at these times the ratio t/Kn is no longer $\ll 1$. Thus, the observed discrepancy may be attributed to the cumulative effect of molecular collisions.

To study the validity of the present analysis to lower Knudsen number flows, figure 3 presents a comparison of the time evolution of the density and velocity perturbations at a fixed location ($x = 0.25$) with DSMC calculations at various Knudsen numbers for both $R_\epsilon = \pm 1$ cases. The wave-like time variation of the hydrodynamic properties is visible. The wave magnitude, however, is rapidly damped and equilibrium is achieved after few acoustic times. The agreement with the $Kn = 10$ results is very good at all

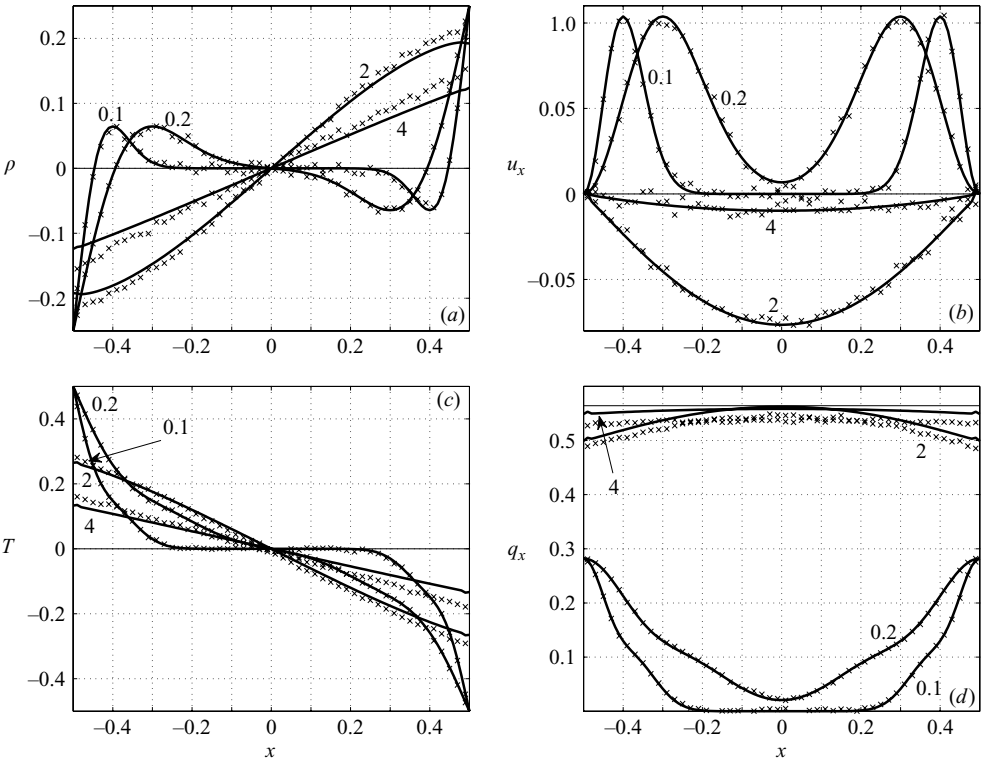

FIGURE 2. (*a*) Density, (*b*) velocity, (*c*) temperature and (*d*) heat-flux perturbation distributions for $R_\epsilon = -1$ and the indicated values of time. The crosses correspond to DSMC results at $Kn = 10$ and the thin solid lines mark the long-time collisionless limit.

times presented. With decreasing Kn (and thus longer t^* corresponding to the same value of the non-dimensional time t) we expect the agreement to become confined to lower values of t owing to the increasing effect of collisions. We thus regard the close agreement in the $Kn = 1$ case for $R_\epsilon = 1$ up to $t = 2$ as remarkable, and perhaps fortuitous. Nevertheless, the existence of an initial time interval $t \lesssim Kn$ where the collisionless analysis is valid is clearly demonstrated.

The latter observation suggests that the present analysis may be useful in providing a quantitative description of the initial transient in the counterpart continuum-limit problem. Figure 4 demonstrates this by presenting a comparison of the early-time behaviour of the velocity and temperature perturbations with DSMC results in the vicinity of the left ($x = -0.5$) wall for $Kn = 0.1$. We note again that at the early times presented the exact collisionless solutions (2.21)–(2.22) and the approximate expressions (2.26)–(2.27) are indistinguishable. These, in turn, are in good agreement with the DSMC data for the cases where $t < Kn$. At the latest time shown, $t = 0.12 > Kn$, the discrepancies due to molecular collisions are already visible.

As mentioned in the introduction, previous continuum analyses have so far based their solutions upon the assumption that the changes in the temperature of the boundaries are gradual so that the use of a kinetic approach is avoided. However, when considering the 'instantaneous-jump' problem (or problems where the time scale for temperature changes is shorter than the mean free time), the molecular character of the gas must be taken into account. In this case, the present analysis

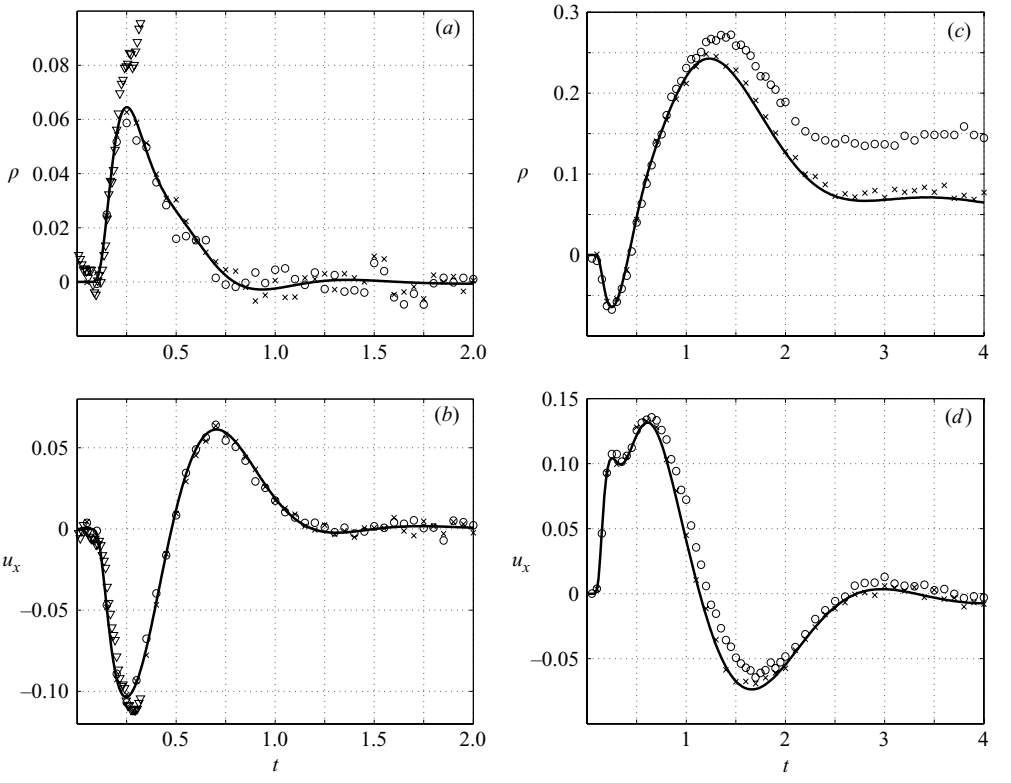

FIGURE 3. Time evolution of the density and velocity perturbations at $x = 0.25$ for $R_\epsilon = 1$ (a, b) and $R_\epsilon = -1$ (c, d). The crosses and circles respectively correspond to DSMC results at $Kn = 10$ and 1. The triangles in (a, b) mark the DSMC solution at $Kn = 0.1$. Recall that, strictly, the collisionless solution is expected to be valid for $t \ll Kn$.

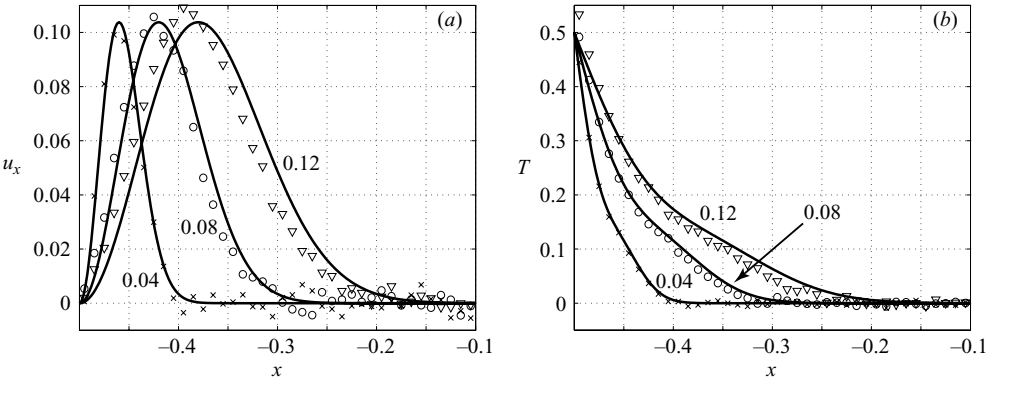

FIGURE 4. Initial transient behaviour of (a) velocity and (b) temperature perturbation fields for $R_\epsilon = 1$ at the indicated values of time. The solid lines correspond to the early-time approximations (2.26)–(2.27) and the different symbols mark the $Kn = 0.1$ DSMC results at $t = 0.04$ (crosses), 0.08 (circles) and 0.12 (triangles).

provides a quantitative description for $t \lesssim Kn$. With increasing t, the cumulative effect of collisions should be considered until finally, at times larger than few collision times, the Navier–Stokes description becomes valid. Future work will concentrate on clarifying these issues.

REFERENCES

Bird, G. 1994 *Molecular Gas Dynamics and the Direct Simulations of Gas Flows*. Clarendon.

Chen, G. 2002 Ballistic-diffusive equations for transient heat conduction from nano to macroscales. *J. Heat Transfer* **124**, 320–328.

Clarke, J. F., Kassoy, D. R. & Riley, N. 1984 Shock waves generated in a confined gas due to rapid heat addition at the boundary. II Strong shock waves. *Proc. R. Soc. Lond.* A **393**, 331–351.

Grad, H. 1958 Principles of the kinetic theory of gases. *Handbuch der Physik*, vol. 12, pp. 205–294.

Hadjiconstantinou, N. G. 2006 The limits of Navier-Stokes theory and kinetic extensions for describing small-scale gaseous hydrodynamics. *Phys. Fluids* **18**, 11130.

Hadjiconstantinou, N. G., Garcia, A. L., Bazant, M. Z. & He, G. 2003 Statistical error in particle simulations of hydrodynamic phenomena. *J. Comp. Phys.* **187**, 274–297.

Ho, C. M. & Tai, Y. C. 1998 Micro-Electro-Mechanical Systems and fluid flows. *Annu. Rev. Fluid. Mech.* **30**, 579–612.

Kogan, M. N. 1969 *Rarefied Gas Dynamics* Plenum.

Lees, L. 1965 Kinetic theory description of rarefied gas flow. *J. Soc. Ind. Appl. Maths* **13**, 278–311.

Patterson, G. N. 1971 *Introduction to the Kinetic Theory of Gas Flows*. University of Toronto Press.

Perlmutter, M. 1967 Analysis of transient heat transfer through a collisionless gas enclosed between parallel plates. *ASME Paper* 67-HT-53.

Radhwan, A. M. & Kassoy, D. R. 1984 The response of a confined gas to thermal disturbance: rapid boundary heating. *J. Engng Maths* **18**, 133–156.

Schlichting, H. 1960 *Boundary Layer Theory*. McGraw-Hill.

Sone, Y. 1965 Effect of sudden change of wall temperature in rarefied gas. *J. Phys. Soc. Japan* **20**, 222–229.

Tzou, D. Y. 1997 *Macro-to-Microscale Heat Transfer*. Taylor and Francis.

Tzou, D. Y., Beraun, J. E. & Chen, J. K. 2002 Ultrafast deformation in Femptosecond laser heating. *J. Heat Transfer* **124**, 284-292.

Wadsworth, D. C., Erwin, D. A. & Muntz, E. P. 1993 Transient motion of a confined rarefied gas due to wall heating or cooling. *J. Fluid Mech.* **248**, 219–235.